Chemistry & Biology
Article

The Mechanostability of Isolated Focal Adhesions Is Strongly Dependent on pH

Kristin Grant Beaumont[1] and Milan Mrksich[1,*]
[1]Departments of Biomedical Engineering, Chemistry, and Cell & Molecular Biology, and Howard Hughes Medical Institute, Northwestern University, Chicago, IL 60208, USA
*Correspondence: milan.mrksich@northwestern.edu
DOI 10.1016/j.chembiol.2012.04.016

SUMMARY

This report demonstrates that the mechanical stability of focal adhesions exhibits a biphasic and sensitive pH dependence. These studies used isolated focal adhesions, which retain many of the properties of the intracellular structures, including protein composition and force-dependent reinforcement by cytosolic proteins. The focal adhesion structures are least stable to applied force at a pH of 6.4, and significantly more stable at slightly higher and lower pH values. This trend is consistent with previous work that characterized the pH dependence of cell migration and may therefore be relevant to controlling the invasiveness of metastatic cancer cells. This approach is significant because it allows biochemical studies of large protein complexes previously studied only in cell culture, and therefore offers new opportunities for performing mechanistic studies of a range of factors that contribute to focal adhesion stability.

INTRODUCTION

The remodeling, or turnover, of focal adhesions is a key step, and sometimes the rate-determining step, in the migration of cells (Palecek et al., 1998). Focal adhesions are complex and still incompletely defined structures and their turnover is highly dynamic and dependent on several factors, including the phosphorylation states of resident proteins and the forces applied by the cytoskeleton. Cells are exposed to in vivo forces on the order of 1–10 nN per cell contact, with small variations in this force causing changes in cell behavior (Chen et al., 2004). Intracellular pH, which is regulated by the plasma membrane Na^+/H^+ exchanger NHE-1, also contributes significantly to the stability and turnover of focal adhesions (Denker and Barber, 2002; for reviews, see Putney et al., 2002; Casey et al., 2010). In addition to its role in migration of healthy cells, the effect of intracellular pH on focal adhesions may have a special significance in cancer biology. One hallmark of cancer cells is their reversed pH gradient—the intracellular pH in normal cells is lower than the surrounding extracellular pH, whereas in cancerous cells, the intracellular pH is higher than the surrounding extracellular pH (Gerweck and Seetharaman, 1996). The reversed pH gradient is thought to facilitate cancer metastasis, as previous studies have shown that cells migrate more readily (with respect to both speed and mean distance traveled) under basic intracellular conditions (Stock et al., 2005) and protease secretion increases under acidic extracellular conditions (Stock and Schwab, 2009). This combination of factors could support the invasiveness of metastatic cancer cells by increasing the dynamic turnover of focal adhesions, leading to more rapid migration, and by increasing the degradation of the surrounding extracellular matrix (Gerweck and Seetharaman, 1996; Izumi et al., 2003; Cardone et al., 2005; Harguindey et al., 2005).

The effect of pH on the structure and stability of the focal adhesion is largely uncharacterized, although several focal adhesion proteins have activities or conformations that are known to be sensitive to pH, and it is also known that the pH regulator, NHE-1, specifically localizes to focal adhesions. For example, the affinity of talin for F-actin is pH sensitive (Goldmann et al., 1999; Schmidt et al., 1999; Srivastava et al., 2008) as are the actin-binding protein alpha-actinin and possibly the conformation and self-association of vinculin (Condeelis and Vahey, 1982; Miller and Ball, 2001; Palmer et al., 2008).

Studies of the effect of pH on focal adhesion structure and stability are most commonly performed in live cell culture and remain challenging. One reason for this is the spatiotemporal variation of intracellular pH—which makes measurement of the average pH a poor substitute for the pH that a focal adhesion experiences locally. Further, it remains difficult to control, or to vary, the intracellular pH. A common strategy to do so relies on adjusting the extracellular pH—which is expected to translate to a change in the intracellular pH—but a variety of other factors influence intracellular pH. Also, the common pH-sensitive dyes that are used to measure intracellular pH (including 2′,7′-bis(2-carboxyethyl)-5(6)-carboxyfluorescein (BCECF) or carboxy SNARF-1) require a complex (and often unreliable) calibration procedure (Chow and Hedley, 1997) that may complicate comparison of absolute intracellular pH values. Moreover, these dyes may be cytotoxic or require damaging introduction techniques (Han and Burgess, 2010). Genetic methods can be used to engineer cells to introduce NHE-1 mutants (Denker et al., 2000; Denker and Barber, 2002), but compensation mechanisms in the cell can confound the effects of experimental factors on intracellular pH.

In this report, we describe a method that circumvents these challenges by isolating focal adhesions from the remainder of

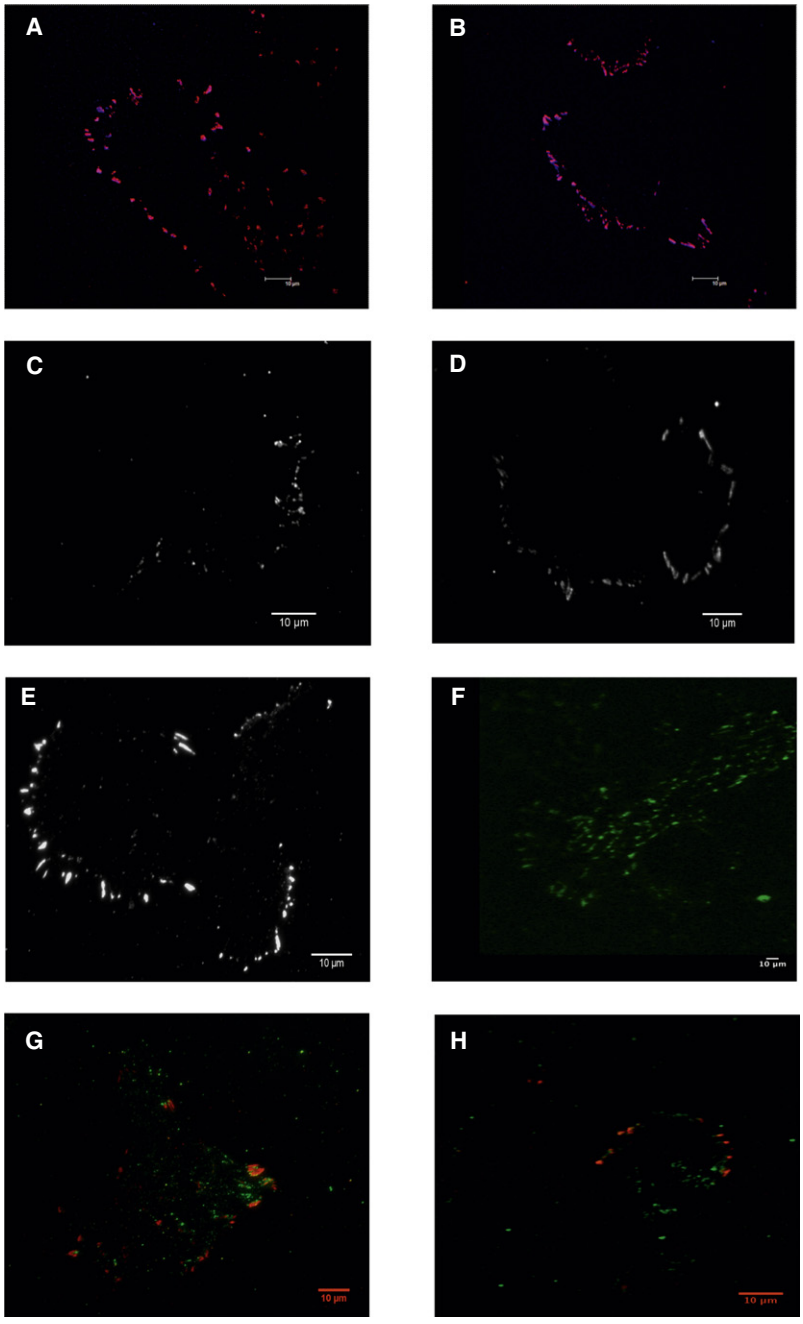

Figure 1. Isolated Focal Adhesions Include the Same Proteins as Focal Adhesions Found in Intact Cells

Isolated focal adhesions were immunostained for a subset of focal adhesion proteins.

(A and B) Confocal fluorescence microscopy images of immunostained isolated focal adhesions demonstrating the presence of talin (red) and actin (blue) (A) and paxillin (red) and actin (blue) (B).

(C–H) Epifluorescent microscopy images demonstrating the presence of FAK (C), phosphorylated FAK (D), vinculin (E), alphaV integrin (F), fibronectin (green) colocalized with vinculin (red) (G), and cell membrane (green) colocalized with vinculin (red) (H).

the cell such that they can be studied in buffers of desired pH. We isolated focal adhesions from cultured cells and then characterized the mechanical properties of the structures in this controlled-pH environment. This method allows us to specifically investigate the pH-dependent mechanostability of focal adhesion complexes, independent of significant extracellular or cytoskeletal contributions. Our work demonstrates that the mechanical properties of focal adhesions are significantly dependent on pH—they are stabilized at low pH values (5.2–5.6) and high pH values (7.2–7.6)—and the stability is affected significantly over a narrow window of physiologically relevant pH.

RESULTS AND DISCUSSION

Preparation and Characterization of Isolated Focal Adhesions

We isolated focal adhesions from adherent HT1080 human fibrosarcoma cells using a modified osmotic shock procedure. Cells were cultured on untreated glass substrates for 12–16 hr in low glucose DMEM supplemented with 10% FBS, 100 U penicillin, 100 μg streptomycin, and 2 mM L-glutamine; this was sufficient time for the cells to deposit extracellular matrix. The substrates were removed from the medium and rinsed with a stream of ice-cold water, which removed the dorsal membrane, cytosol, and organelles of the cells but left intact focal adhesions on the glass substrate. Related approaches have been explored to isolate cytoskeletal networks from cultured cells (Sawada and Sheetz, 2002), but these studies investigated force-dependent binding of cytosolic proteins to the cytoskeletal network.

We characterized the isolated focal adhesions by immunostaining and verified the presence of several expected focal adhesion proteins including vinculin, talin, paxillin, focal adhesion kinase (FAK), phosphorylated FAK, and alpha V integrin in structures that resembled focal adhesions (Figure 1). Moreover, remnants of actin, cell membrane, and fibronectin were also associated with these structures.

Investigating the Mechanical Properties of Isolated Focal Adhesions

System Setup and Calibration

An electromagnetic microneedle was used to apply forces up to 140 pN to magnetic beads that were attached to the complexes; bead preparation and attachment are discussed in the next section. A representation of magnetic bead-labeled complexes is shown in Figure 2A. The microneedle setup is similar to the one discussed by Ingber and coworkers (Alenghat et al., 2000),

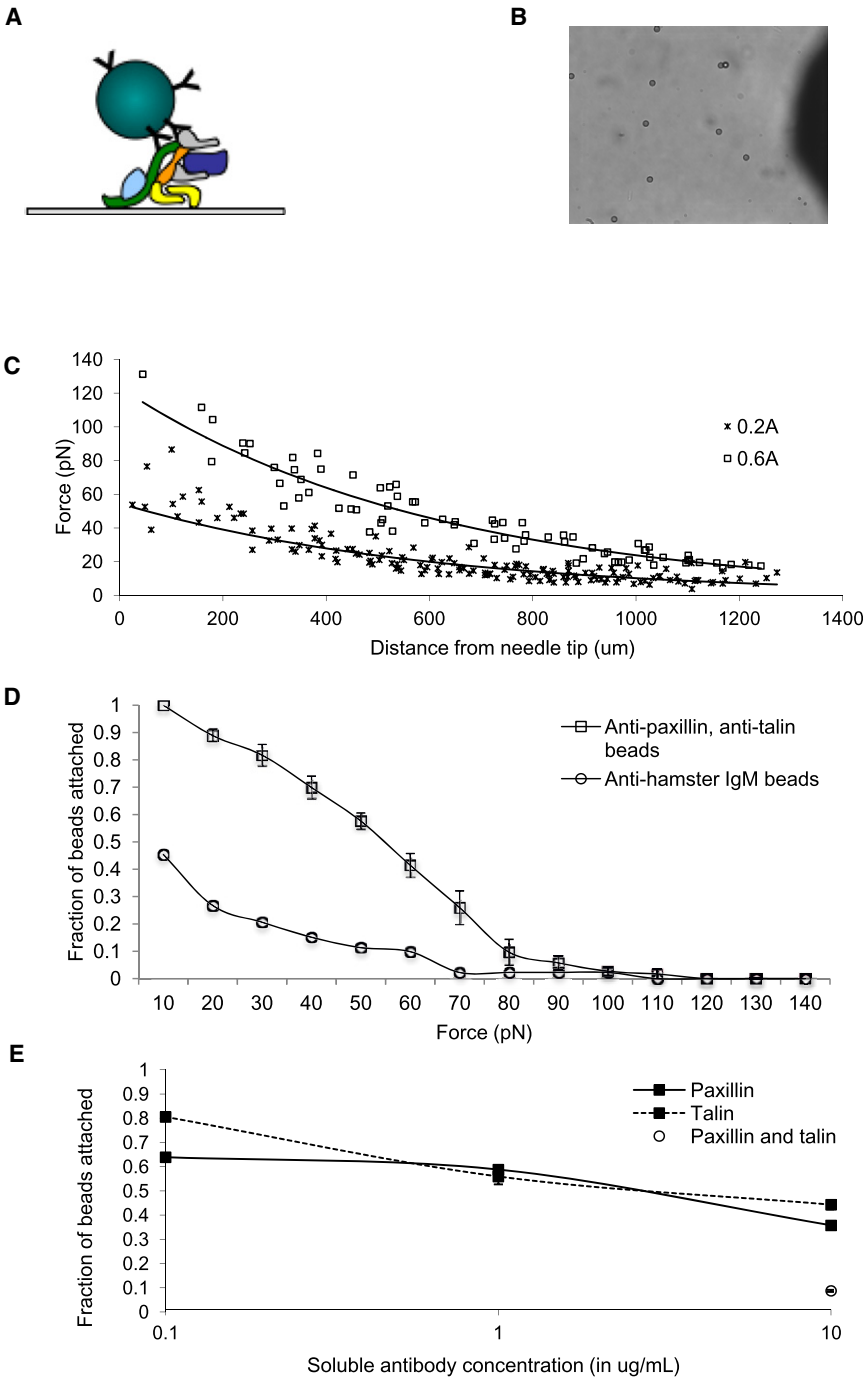

Figure 2. Isolated Focal Adhesions Are Specifically Labeled with Magnetic Beads Presenting Anti-Talin and Anti-Paxillin Antibodies and These Beads Are Mechanically Interrogated with a Calibrated Magnetic Microneedle

(A) Cartoon showing antibody-coated bead specifically attached to paxillin and talin in an isolated focal adhesion.

(B) Brightfield image showing beads (2.8 μm diameter) and needle tip.

(C) Sample calibration curves showing the relationship between the force applied to a bead and its distance from the microneedle tip.

(D) Bead detachment curves showing that magnetic beads conjugated to anti-hamster IgM do not attach to isolated focal adhesions (mean ± SEM).

(E) Competition curves showing that bead attachment is inhibited by the addition of soluble anti-talin and anti-paxillin (mean ± SEM).

and its specifications are detailed in the Experimental Procedures section. Briefly, the magnetic microneedle was fabricated from HyMu magnetic alloy, wrapped with magnetic wire, connected to a 3 A power supply, and mounted to an X,Y,Z micromanipulator, which was in turn mounted to the air table supporting an inverted microscope. The experiments were performed at room temperature, using a HEPES-based buffer. The pH of the test buffer was confirmed at the end of each experiment, and it was found that the pH did not change (<0.05 pH units). As an additional check, the temperature of the sample was confirmed at the end of each experiment, and it, too, did not change (<1°C). A microscopy chamber was used to hold the glass substrate containing the isolated focal adhesions as well as the test buffer. Once the holder was in place on the microscope stage, the needle was brought in from the side, and precisely positioned using the micromanipulator. A brightfield image of the needle after placement near the bead-labeled substrate is shown in Figure 2B.

We performed a series of experiments in order to calibrate the force-distance relationship for the electromagnetic microneedle. Ferromagnetic beads 2.8 μm in diameter were suspended in 100% glycerol. The needle was positioned in the sample holder and its height positioned such that it was the same distance above beads in a focal plane as during actual bead-pulling experiments (2 μm). The test current was applied for 1 min and brightfield images were acquired every second. Each test current (0.2, 0.4, and 0.6 A) was repeated three times. Beads were tracked using the manual tracking feature of ImageJ, and their velocities were calculated as a function of distance from the microneedle tip. Stoke's Law was then used to calculate the applied force as a function of bead distance from the needle from the measured bead velocity, glycerol viscosity, and bead diameter. The data from all three trials were combined and fit to an exponential relationship, which was used in subsequent experiments to determine the force experienced by each test bead as a function of its distance from the needle tip. Representative calibration curves are shown in Figure 2C.

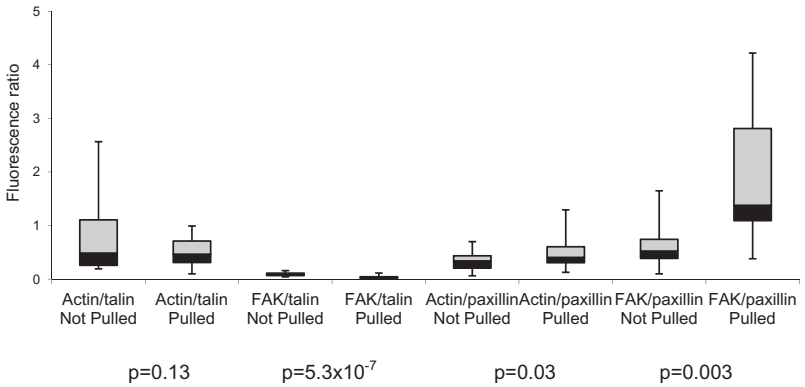

Figure 3. The Mechanical Failure Point of Bead-Labeled Isolated Focal Adhesions Resides within the Focal Adhesion, Not between the Bead-Conjugated Antibody and Its Target Protein

Box-and-whisker plot showing how the ratio of various focal adhesion proteins changes after bead-labeled isolated focal adhesions are pulled to failure, demonstrating that beads are removed because of disruption of protein-protein interactions within the focal adhesion, as opposed to disruption of the interactions between the antibodies on the beads and their focal adhesion target proteins. This plot suggests a model where bead detachment causes the removal of both paxillin and FAK, but not talin.

Bead Preparation and Attachment to Isolated Focal Adhesions

In order to attach the beads to the isolated focal adhesions, we covalently modified the beads with antibodies against talin and paxillin, as described in Experimental Procedures. The beads specifically associated with the isolated focal adhesions, as shown by two control experiments (Figures 2D and 2E). First, beads that were coated at the same density with mouse anti-hamster IgM, which does not recognize focal adhesion proteins, largely failed to attach to the isolated focal adhesions; of those that did, greater than 80% were removed by 30 pN of force (Figure 2D). The attachment of beads was also inhibited by the addition of soluble anti-paxillin and anti-talin antibodies in a dose-dependent manner (Figure 2E). This inhibition experiment also demonstrated that both antibodies contributed approximately equally to binding of the beads to isolated focal adhesions.

In a typical experiment, we bring the microneedle into the vicinity of the bead-labeled focal adhesions and increase the applied force in steps (by increasing the current from 0.2 A to 0.4 A to 0.6 A, where each current was applied for 1 min), allowing the number of beads that remain attached to the substrate after each step to be counted. Beads farthest away from the needle typically experience forces over the range of 10–40 pN, and beads close to the needle experience forces over the range of 50–140 pN. We present data by recording the force at which each bead attached and plotting the fraction of beads that remain attached with each 10 pN increase in applied force. We image six fields of view per trial, where each field typically included four to six beads and we perform three or four trials for each experimental condition to obtain data for approximately 100 beads. The detachment curves shown in each of the figures in this work represent an average of the data from each trial.

We used the force at which the bead detached from the isolated focal adhesion as a measure of its stability. To confirm that the bead detachment was due to disruption of protein-protein interactions within the focal adhesion—and not of the immobilized antibody and proteins in the focal adhesion—we performed several control experiments. First, we analyzed the composition of the focal adhesions that remained after the beads were magnetically detached from the substrate. The substrates were fixed and immunostained for several focal adhesion proteins; one set was stained for FAK, actin, and talin, and the other set was stained for FAK, actin, and paxillin. We used antibodies that were labeled with three resolvable fluorophores so that protein levels could be accurately ratioed within each focal adhesion. Laser scanning confocal images were acquired from 20 separate fields of view in the area where beads had been removed. We also performed these experiments for bead-conjugated samples that were not subjected to force to compare the compositions of the focal adhesions prior to force application. In this way, we could determine the relative amounts of proteins within the focal adhesions (by using ratios of fluorescence intensity for samples that were immunostained for two different components) and estimate the relative amounts of each protein before and after bead removal; since staining with antibodies raised in mouse (talin and paxillin) was the crispest, signal from the other proteins was ratioed against either talin or paxillin.

These experiments revealed that bead removal results in changes to the relative amounts of focal adhesion proteins (Figure 3), demonstrating that beads are removed because of disruption of protein-protein interactions within the focal adhesion, as opposed to disruption of the interactions between the antibodies on the beads and their focal adhesion target proteins. Specifically, the ratio of actin to talin does not change significantly after bead removal ($p = 0.13$), suggesting that these proteins remain associated with the focal adhesion (or bead) to comparable extents after removal of the bead. The amount of FAK that remains associated with the focal adhesion, in contrast, decreases dramatically relative to talin after removal of the bead ($p = 5.3 \times 10^{-7}$), suggesting that the focal adhesion does not remain fully intact following bead removal. Further, we find that the ratio of actin to paxillin shows a statistically significant increase following bead removal ($p = 0.03$). These experiments suggest that the amounts of both paxillin and FAK decrease in the isolated focal adhesions after removal of the bead, but that paxillin decreases to a much greater extent than does FAK. This interpretation is also consistent with a similar experiment showing that the ratio of FAK to paxillin increases significantly ($p = 0.003$) after removal of the beads. These trends are reasonable in that they are consistent with a model in which the removed bead is associated with more paxillin than FAK, but not more talin, which is known to associate with β1 integrin and reside primarily at the basal region of the focal adhesion (Zamir and Geiger, 2001).

Isolated Focal Adhesions Exhibit Specific Mechanical Reinforcement in the Presence of Cell Lysate

We demonstrated the physiological relevance of these isolated focal adhesion structures by showing that they exhibit a key

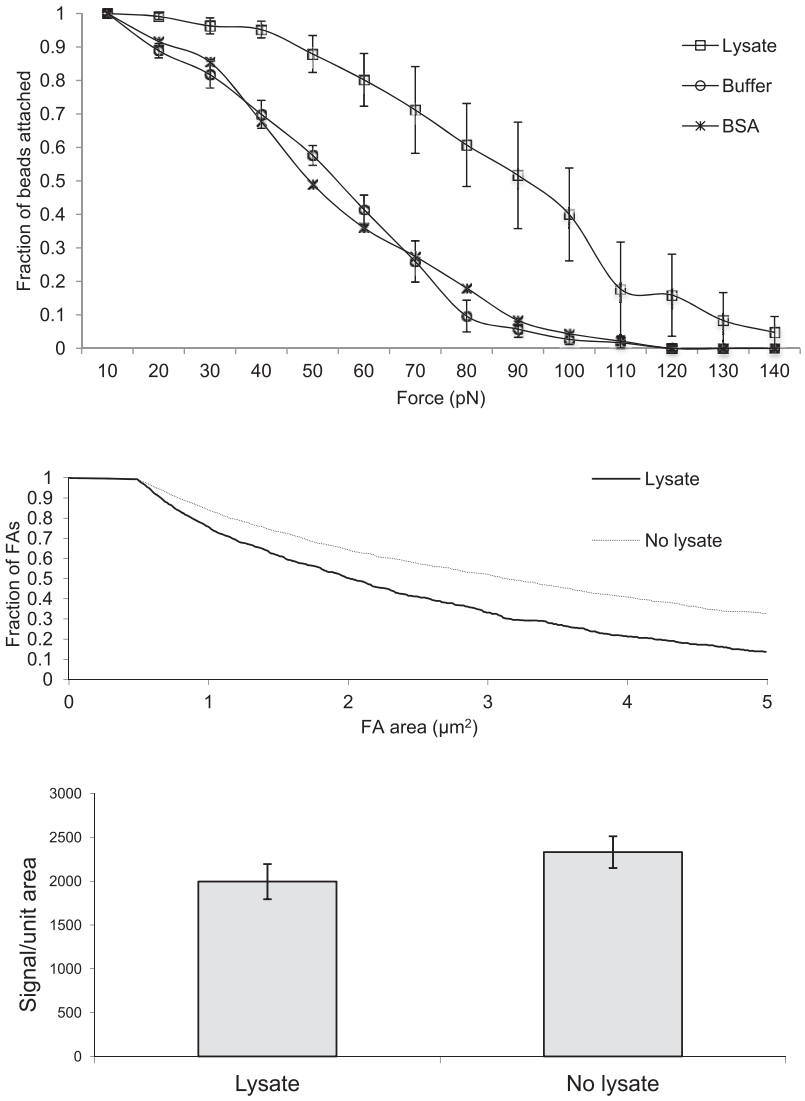

Figure 4. Isolated Focal Adhesions Are Mechanically Reinforced in the Presence of Cytosolic Proteins

(Top) Bead detachment curves showing specific focal adhesion reinforcement due to cell lysate proteins (mean ± SEM). This plot shows that beads are considerably more resistant to removal in the presence of HT1080 cell lysate, but not in the presence of the same concentration of bovine serum albumin.

(Middle) Cumulative probability plot showing the size distribution of isolated focal adhesions (as determined by immunostaining for paxillin) in the presence and absence of HT1080 cell lysate without force application.

(Bottom) Plot showing the fluorescence intensity of paxillin per unit area for isolated focal adhesions incubated with HT1080 cell lysate (left) and buffer (right), both in the absence of force (mean ± SD). This plot shows no statistically significant difference between these two populations.

behavior of native cellular focal adhesions; they undergo reinforcement due to protein recruitment (Riveline et al., 1999; Balaban et al., 2001). We used the electromagnetic microneedle to apply forces up to 140 pN to bead-tagged focal adhesions in the presence of HT1080 cell lysate and observed that the beads were considerably more resistant to detachment when pulled in 0.2 mg/ml cell lysate as compared to buffer (shown in Figure 4). We found that the number of beads that remained attached to the focal adhesions under a 60 pN force approximately doubled when the experiment was performed in cell lysate (0.2 mg/ml) relative to a buffer. This reinforcement effect was not observed when the lysate was substituted with a buffer containing 0.2 mg/ml BSA. Moreover, we performed a control experiment that demonstrates that the observed reinforcement is not simply due to an increase in bound focal adhesion proteins from the cell lysate. We characterized isolated (non-bead-labeled) focal adhsions by immunostaining after exposure to 0.2 mg/ml HT1080 lysate, in the absence of applied force. We found that both the sizes and fluorescent intensities of paxillin-containing focal adhesions actually showed a slight decrease upon addition of cell lysate in the absence of applied force (Figure 4). Therefore, the observed reinforcement cannot be simply ascribed to passive protein binding to the isolated focal adhesions. Our observation of the force-dependent reinforcement effect is consistent with previous studies that showed that the elastic stiffness of individual magnetic-bead-tagged focal adhesions in intact cells increased due to local focal adhesion assembly (Matthews et al., 2004, 2006). This finding, together with the immunostaining experiments, suggest that these isolated focal adhesions possess many of the properties of intracellular focal adhesions. While this system does not capture all of the nuances of the cellular structures—their composition may not correspond completely or they may exhibit altered dynamic properties—we believe that they represent an important contribution to the existing methods that can be used to study their mechanical properties.

The Mechanical Properties of Isolated Focal Adhesions Are pH Sensitive

We next repeated the bead-pulling experiment using buffers that had pH values ranging from 5.2 to 7.6, and which represent values that could be reasonably expected for localized regions in normal or cancerous cells (Griffiths, 1991; Gerweck and Seetharaman, 1996; Casey et al., 2010). In all experiments, the magnetic beads were prepared as described above and allowed to attach to the surfaces presenting isolated focal adhesions in a buffer adjusted to a pH of 7.0. Once the beads had attached, the surfaces were rinsed (to remove free beads), treated with buffer that had a designated pH, and mechanically probed as described above. The data were again binned in 10 pN increments and presented as described above. For each pH value, more than 95% of the beads remained attached at 10 pN, and

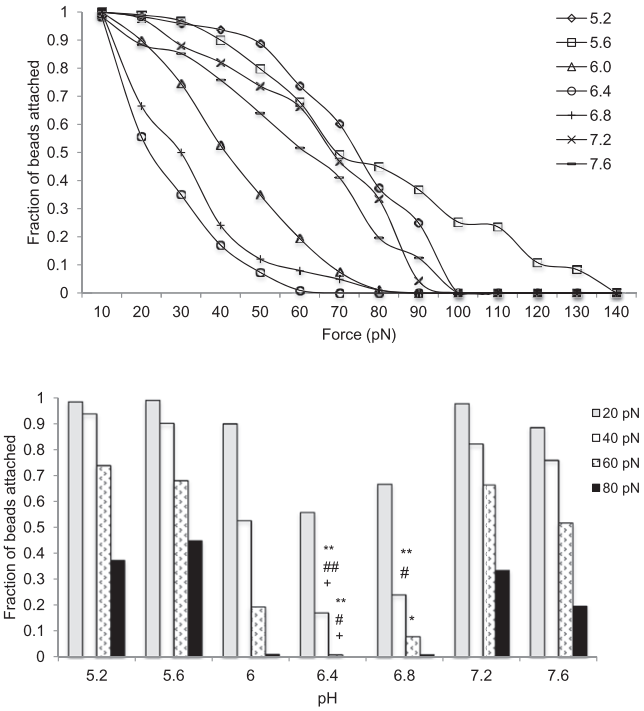

Figure 5. The Mechanical Stability of Isolated Focal Adhesions Exhibits a Biphasic Dependence on pH

(Top) Bead detachment curves showing the fraction of beads attached as a function of applied force over different pH conditions.

(Bottom) Data reconfigured to clarify the effect of pH at several key forces. Statistical significance is represented as follows: *, comparison to pH 5.2; #, comparison to pH 5.6; +, comparison to pH 7.2. P value is represented by the number of each symbol: one symbol denotes $p < 0.05$ and two symbols denote $p < 0.01$ (e.g., ++ denotes $p < 0.01$ compared to the same force at pH 7.2).

all of the beads detached after application of a force of 140 pN to the complexes.

The detachment curves reveal that the number of beads that are removed from the substrate—and which we define as a measure of focal adhesion stability—increases rapidly with low forces when buffers of intermediate pH are used, whereas higher forces are required to disrupt the focal adhesions in buffers that have higher and lower values of pH. These curves show that the focal adhesions are most stable in buffers with values of below pH 6.0 and above 7.2. In contrast, focal adhesions in buffers with pH values of 6.4 and 6.8 are substantially destabilized. We repeated these experiments a sufficient number of times to give statistically meaningful comparisons of the stabilities of focal adhesions at different values of pH; four randomized replicates were performed for each pH, with each replicate consisting of six fields of view (with four to six beads per field), for a total of approximately 100 beads analyzed per pH condition. A comparison of the fraction of beads that remained attached after application of a 60 pN force gives a clear indication of the biphasic and sensitive dependence of focal adhesion stability on pH (Figure 5). For example, after application of 60 pN, 74% ± 14% (mean ± SEM) of beads remained attached at pH 5.2 and 52% ± 20% of beads remained attached at pH 7.6, but under the same force-application conditions at pH 6.4, only 1 ± 1% of beads remained attached. This trend in pH-dependent stability also extends over a range of applied forces. For example, a comparison of the bead-detachment curves at values of pH 5.6 and 6.4 demonstrates that the number of beads that remained associated with the focal adhesions was significantly different after application of forces of 40 pN ($p < 0.01$) and 60 pN ($p < 0.05$); similarly, the stability of adhesions at pH 6.4 and 7.2 was significantly different after application of 40 pN ($p < 0.05$) and 60 pN ($p < 0.05$). Taken together, these results show that focal adhesion stability exhibits a striking dependence on pH over a narrow window of physiologically relevant pH values (5.2–7.6). These observations are consistent with the disruption of protein interactions within the isolated focal adhesion, which, due to the sharp nature of the pH dependence, is likely cooperative.

We performed a series of immunoprecipitation experiments to rule out the possibility that these trends are due to a pH-dependent binding of the immobilized antibodies to their target proteins. In these experiments, cell lysates were prepared from HT1080 cells and incubated with anti-talin- and anti-paxillin-conjugated magnetic beads, identical to those used in bead-pulling experiments. Binding was performed in pH 7.0 buffer, and then the beads were rinsed in buffer at the desired pH, in the same manner as in bead-pulling experiments. The protein was separated from the beads by boiling and a western blot was run on the supernatant, where GAPDH was used as a loading control. The intensity of each paxillin or talin band was ratioed against its corresponding GAPDH band. Three independent replicates of this experiment were performed, and they demonstrated that the antibody-conjugated beads bound statistically similar amounts of paxillin and talin at all values of pH that were tested (Figure 6). These experiments suggest that anti-paxillin and anti-talin antibodies bind to their target proteins with the same affinity at each of the pH test conditions in this work.

We performed another experiment to address the possibility that the structure of the focal adhesion changes with pH in a force-independent manner. We incubated substrates presenting isolated focal adhesions in three different buffers (having pH values of 5.2, 6.4, and 7.2), fixed the samples, and stained for paxillin as a marker of focal-adhesion size. We found that neither the size nor the amount of paxillin in the focal adhesion (as measured by fluorescence intensity) changed as a function of pH (Figure 7). Taken together, these data suggest that isolated focal adhesion stability is dramatically affected by pH, and this effect cannot be ascribed to pH-dependent bead binding to the focal adhesions or pH-dependent structural changes in the isolated focal adhesions.

The trends demonstrated here are particularly interesting in the context of previous cell migration studies. It is challenging to compare our observations to other data at absolute pH values (due to the uncertainty in the fluorescence methods used to measure intracellular pH, as described above), but drawing parallels between observed trends in our work and in the cell-migration literature is both warranted and useful. Of particular note are similarities to reports describing biphasic trends in cell migration and focal-adhesion turnover/cell migration which is very sensitive to small (<0.5 units) pH changes.

As an example, the migration rate of melanoma cells was found to depend on extracellular pH (pH_e) (Stock et al.,

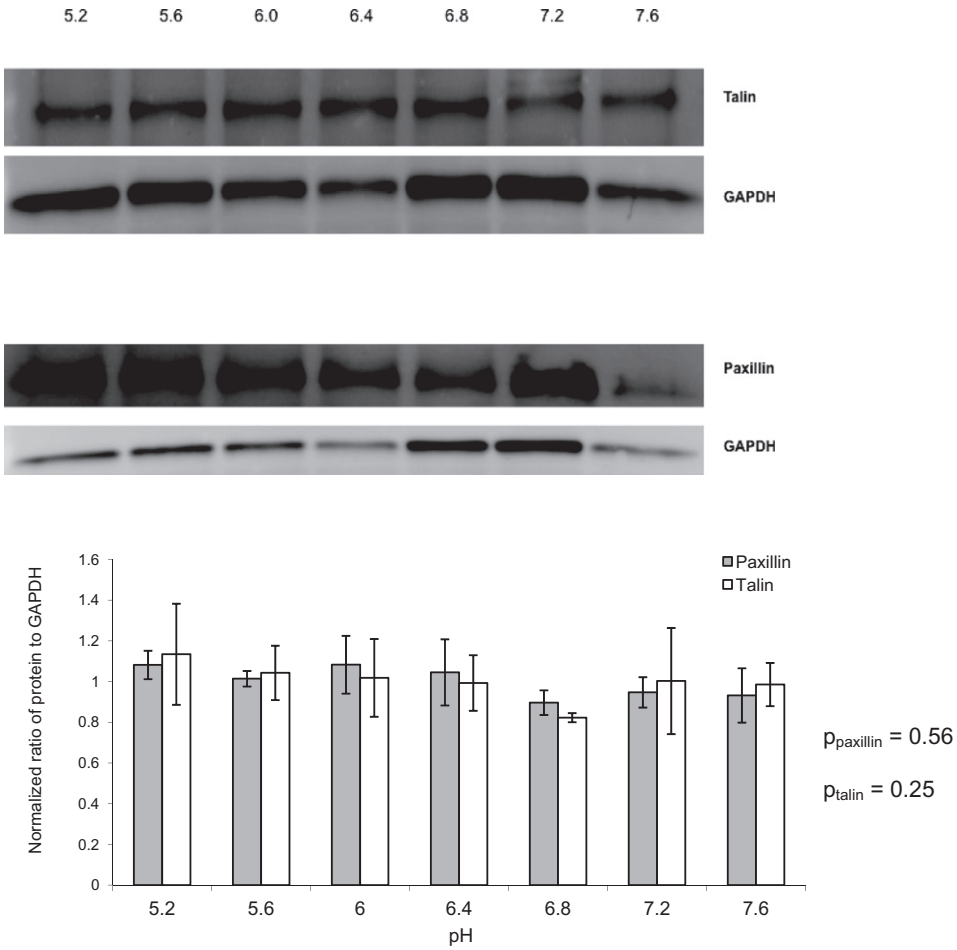

Figure 6. Bead Binding of Paxillin and Talin Does Not Vary as a Function of pH

(Top) Representative western blots of supernatant resulting from immunoprecipitation of paxillin and talin from cell lysate with anti-talin- and anti-paxillin-conjugated beads at each experimental pH value showing bands attributable to talin (~225 kDa) and paxillin (~68 kDa) and their respective GAPDH bands, which were used as loading controls.

(Bottom) Plot showing the ratio of talin or paxillin band intensity to its respective GAPDH band intensity. Bars are an average of three independent replicates (mean ± SD) and ANOVA analysis reveals no statistically significant difference among pH values.

2005). These cells exhibited a greater migration rate at a pH_e of ~7.0, than they did at either higher or lower pH_e values (7.5 and 6.6 respectively). This biphasic dependence was explained by a pH dependence of the cell-matrix interactions (specifically between integrin receptors and collagen I) and carried the reasonable inference that migration would be impeded by interactions that were either too strong (at acidic pH) or too weak (at basic pH). Other work showed that integrin-dependent migration of neutrophils was greatest at a pH_e of 7.4 but again significantly decreased in the presence of buffers with lower (6.2–6.8) or higher (8.3–8.6) pH_e values (Simchowitz and Cragoe, 1986; Jannat et al., 2010). This and other work reveals that cell migration is most rapid at neutral pH and decreases at both more acidic and more basic pH, but has not established the mechanistic basis for this pH dependence. While other factors, such as pH-dependent integrin avidity could contribute to this effect, our results suggest that pH-dependent focal adhesion stability could also be a contributing cause to the biphasic relationship between cell migration and pH.

Our results are also consistent with a body of very interesting work done by Barber and colleagues, which showed striking sensitivity of focal adhesion stability to small pH changes (Tominaga and Barber, 1998; Denker et al., 2000; Denker and Barber, 2002; Frantz et al., 2007; Srivastava et al., 2008). In that work, fibroblasts were engineered to express a mutant NHE-1, which impaired ion translocation and resulted in a cytosolic pH that was approximately 0.2–0.3 units lower than wild-type (WT) cells (~7.0 versus ~7.3). Accumulation of focal adhesion proteins, including vinculin and paxillin, was impaired in these cells and the rates of cell migration were significantly slower as compared to WT cells (~3 μm/hr versus ~19 μm/hr for WT). The authors concluded that the rate-determining step for the decreased migration was impaired trailing-edge deadhesion resulting from deficient focal-adhesion turnover. A subsequent study (Denker and Barber, 2002) showed that the NHE-1 mutant cells migrated

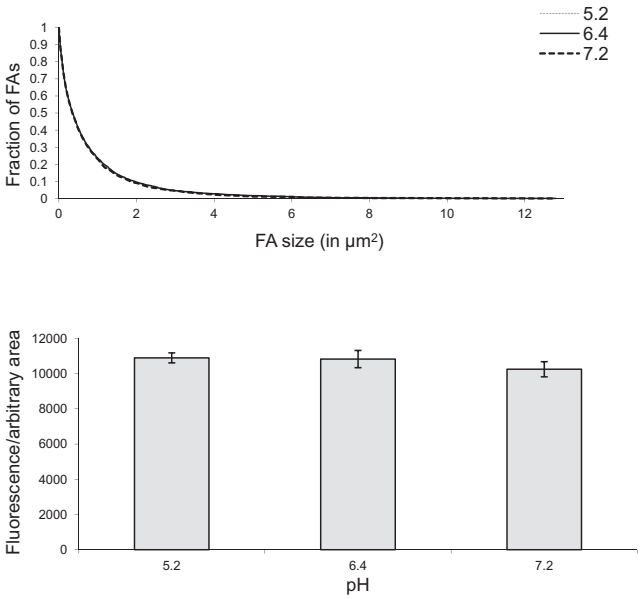

Figure 7. Focal Adhesion Size and Paxillin Content Do Not Change as a Function of pH

(Top) Cumulative probability plot showing that the size distribution of focal adhesions does not change after incubation in buffers of pH 5.2, 6.4, and 7.2.

(Bottom) Plot showing that fluorescence intensity (from paxillin immunostaining) per unit area does not change after incubation in buffers of pH 5.2, 6.4, and 7.2. These results suggest that pH does not affect focal adhesion structure (mean ± SD).

more slowly due to decreased focal-adhesion turnover, which was the result of an increase in affinity of F-actin binding by talin. Taken together, that work is consistent with the present study in that they demonstrate that focal-adhesion structure and stability are highly sensitive to pH changes over a very narrow (<0.5) physiologically relevant window.

SIGNIFICANCE

To our knowledge, this work describes a new strategy for studying the structures and functions of focal adhesion complexes. The isolation of focal adhesions from cultured cells permits control of their immediate biochemical environment in a manner that has been previously unattainable. At the same time, the isolated complexes retain many characteristics of the cellular structures, including the presence of resident proteins and the force-dependent reinforcement by cytosolic proteins. We used this system to study the effect of pH on focal adhesion complex stability. Unlike studies performed with live cell culture, our approach allowed unambiguous control over the pH and could characterize large numbers of complexes to give statistically meaningful data. The finding that isolated focal adhesion stability shows a biphasic dependence that is highly sensitive to pH agrees with previous studies in the cell-migration literature. Our approach reveals a striking sensitivity of isolated focal adhesion stability to pH, suggesting that local control of pH is important to maintaining appropriate focal adhesion dynamics. We believe that the approach described here will be similarly important for investigating a host of other focal adhesion activities.

EXPERIMENTAL PROCEDURES

Cell Culture and Lysate Production

HT1080 fibrosarcoma cells (CCL-121: ATCC) were maintained in low-glucose DMEM supplemented with 10% FBS, 100 U penicillin, 100 μg streptomycin, and 2 mM L-glutamine (Invitrogen) at 37°C in 5% CO_2. Cells were seeded at a density of 10,600 cells/cm^2 on 40 mm round glass coverslips (clean but untreated) and allowed to spread for 12–16 hr in fully supplemented media. HT1080 lysate was generated by lysing confluent cells on ice for 30 min in buffer containing the following: 1 mM EDTA, 1 mM EGTA, 10 mM Tris, 1 mM $MgCl_2$, 154 mM KCl, 1x Complete Mini Protease Inhibitor Cocktail (Roche Diagnostics, Indianapolis, IN), 15 mM DL-dithiothreitol (DTT), and 0.1% Triton-X.

Focal-Adhesion Isolation, Maintenance, and Bead Labeling

Focal adhesions were isolated from adherent, subconfluent, early-passage HT1080 fibrosarcoma cells by rinsing the substrate vigorously in a stream of ice-cold water. Isolated focal adhesions were maintained in buffer composed of the following: 25 mM HEPES (pH 7.0), 2.5 mM $MgCl_2$, 1 mM $CaCl_2$, 125 mM KCO_2CH_3, and 12 mM glucose (noted as HCB buffer) (Cattelino et al., 1999). For pH studies, the HCB buffer was brought to the appropriate pH value using either HCl or KOH immediately prior to use.

Isolated focal adhesions were stained with the following antibodies: rabbit anti-human focal adhesion kinase (pp125^{FAK}: Sigma-Aldrich), rabbit anti-human phosphorylated FAK (pTyr^{397}: Sigma-Aldrich, St. Louis, MO), mouse anti-human vinculin (clone hVIN-1: Sigma-Aldrich), mouse anti-human paxillin (clone 5H11: Upstate/Millipore, Billerica, MA), and mouse anti-human talin (clone 8d4: Sigma-Aldrich). Alexafluor secondary antibodies were used for visualization (Invitrogen, Carlsbad, CA). Texas red-phalloidin (Invitrogen) was used for actin staining.

Mouse anti-human paxillin (2 μg) and mouse anti-human talin (0.9 μg) were covalently conjugated to 2.8-μm-diameter, superparamagnetic carboxylic-acid-terminated Dynabeads (Invitrogen) using N-Ethyl-N′(3-dimethylaminopropyl)carbodiimide (EDC: Sigma-Aldrich) coupling. These loading parameters were chosen based on the masses of the antibodies, to result in beads presenting equal parking areas for paxillin and talin. Mouse anti-hamster IgM (clone HG-31: Sigma-Aldrich) was used to coat control beads at the same total protein loading concentration (2.9 μg). Isolated focal adhesions were labeled at pH 7.0 with 1.2 × 10^5 beads/cm^2 for 20 min at room temperature. The surface was agitated with buffer at the desired pH to remove nonspecifically attached beads, and fresh buffer was applied for the bead pulls.

Magnetic Microneedle Apparatus and Bead-Pulling Experiments

The magnetic microneedle was fabricated from HyMu magnetic alloy (MuShield, Londonberry, NH) with a tip diameter of 10 μm and was wrapped with magnetic wire (7 feet of wire over ~250 turns), connected to a 3 A power supply (VWR International, Radnor, PA), and mounted to an X,Y,Z micromanipulator (Newport Corporation, Irvine, CA), which was in turn mounted to the air table supporting an inverted microscope (Zeiss Axiovert, Oberkochen, Germany). Currents from 0.2–0.6 A were applied, resulting in forces up to 140 pN; the force applied to each individual bead was a function of its distance from the tip of the magnetic microneedle. The relationship between distance from the needle and applied force was calibrated by Stoke's Law using 2.8-μm-diameter beads suspended in 100% glycerol. The experiments were performed in under an hour, and the pH was checked at the conclusion of the experiment to verify that it did not change (<0.05 pH units). Brightfield images were acquired at 100× and image processing was performed in ImageJ (U.S. National Institutes of Health, Bethesda, MD); bead position was tracked using the Manual Tracking plugin. The calibrated distance/force relationship was applied to determine the force sustained by beads while they remained attached, as well as the force that caused bead detachment.

Western Blot Analysis

Confluent P4 HT1080 cells were detached from flasks with 2 mM EDTA and 1 mM EGTA in PBS and lysed on ice in lysis buffer containing 1 mM EDTA, 1 mM EGTA, 10 mM Tris (pH 7.4), 1 mM $MgCl_2$, 154 mM KCL, 1 mM DTT, 1% Triton X-100, and 1× cOmplete Mini protease inhibitor cocktail (Roche). Lysates were incubated with anti-talin/anti-paxillin beads in pH 7.0 HCB with agitation for 20 min, rinsed in pH 5.2, 5.6, 6.0, 6.4, 6.8, 7.2, or 7.6 HCB and then incubated with the same pH buffer with agitation for 20 min. Beads were magnetically separated and resuspended in 50 μl HCB (pH 7.0), mixed with reducing bromophenol blue loading buffer (1:1 v/v), and boiled at 100°C for 10 min. SDS-PAGE was performed using 12% Tris-glycine gels (PAGEr Gold, Lonza, Basel, Switzerland) and a Minigel System (Lonza). Electroblotting was performed at 17 V for 50 min using a semidry transfer unit (Amersham Biosciences, Piscataway, NJ). The nitrocellulose membranes (Genscript) holding the blotted proteins were blocked in 2.5% (v/v) goat serum (Invitrogen) in 0.1% Tween in TBS (TBS-T) overnight at 4°C and then washed with TBS-T. Overnight incubation with the primary antibody (1:1,000) at 4°C in TBS-T was followed by a 2 hr incubation with a horseradish-peroxidase-conjugated secondary antibody (1:1,000) at room temperature in 2.5% goat serum in TBS-T. Blots were developed using an ECL immunoblotting detection reagent kit (GE, Waukesha, WI). Band intensities were quantified in ImageJ (U.S. National Institutes of Health) where the number of pixels at a given intensity were multiplied by that intensity and summed for all of the pixels ascribable to a given band. Bands attributable to paxillin and talin were ratioed against their respective GAPDH bands.

Statistical Analysis

ANOVA was performed to assess statistical significance, which is defined as $p < 0.05$.

ACKNOWLEDGMENTS

This work was funded by the Chicago Biomedical Consortium with support from the Searle Funds at The Chicago Community Trust. This work was also supported by the National Institutes of Health.

Received: December 3, 2010
Revised: April 4, 2012
Accepted: April 6, 2012
Published: June 21, 2012

REFERENCES

Alenghat, F.J., Fabry, B., Tsai, K.Y., Goldmann, W.H., and Ingber, D.E. (2000). Analysis of cell mechanics in single vinculin-deficient cells using a magnetic tweezer. Biochem. Biophys. Res. Commun. *277*, 93–99.

Balaban, N.Q., Schwarz, U.S., Riveline, D., Goichberg, P., Tzur, G., Sabanay, I., Mahalu, D., Safran, S., Bershadsky, A., Addadi, L., and Geiger, B. (2001). Force and focal adhesion assembly: a close relationship studied using elastic micropatterned substrates. Nat. Cell Biol. *3*, 466–472.

Cardone, R.A., Casavola, V., and Reshkin, S.J. (2005). The role of disturbed pH dynamics and the Na^+/H^+ exchanger in metastasis. Nat. Rev. Cancer *5*, 786–795.

Casey, J.R., Grinstein, S., and Orlowski, J. (2010). Sensors and regulators of intracellular pH. Nat. Rev. Mol. Cell Biol. *11*, 50–61.

Cattelino, A., Albertinazzi, C., Bossi, M., Critchley, D.R., and de Curtis, I. (1999). A cell-free system to study regulation of focal adhesions and of the connected actin cytoskeleton. Mol. Biol. Cell *10*, 373–391.

Chen, C.S., Tan, J., and Tien, J. (2004). Mechanotransduction at cell-matrix and cell-cell contacts. Annu. Rev. Biomed. Eng. *6*, 275–302.

Chow, S., and Hedley, D. (1997). Flow cytometric measurement of intracellular pH. In Current Protocols in Cytometry, J.P. Robinson, Z. Darzynkiewicz, R. Hoffman, J. Nolan, P. Rabinovitch, and S. Watkins, eds. (New York: John Wiley & Sons), pp. 9.3.1–9.3.10.

Condeelis, J., and Vahey, M. (1982). A calcium- and pH-regulated protein from *Dictyostelium discoideum* that cross-links actin filaments. J. Cell Biol. *94*, 466–471.

Denker, S.P., and Barber, D.L. (2002). Cell migration requires both ion translocation and cytoskeletal anchoring by the Na-H exchanger NHE1. J. Cell Biol. *159*, 1087–1096.

Denker, S.P., Huang, D.C., Orlowski, J., Furthmayr, H., and Barber, D.L. (2000). Direct binding of the Na-H exchanger NHE1 to ERM proteins regulates the cortical cytoskeleton and cell shape independently of H^+ translocation. Mol. Cell *6*, 1425–1436.

Frantz, C., Karydis, A., Nalbant, P., Hahn, K.M., and Barber, D.L. (2007). Positive feedback between Cdc42 activity and H^+ efflux by the Na-H exchanger NHE1 for polarity of migrating cells. J. Cell Biol. *179*, 403–410.

Gerweck, L.E., and Seetharaman, K. (1996). Cellular pH gradient in tumor versus normal tissue: potential exploitation for the treatment of cancer. Cancer Res. *56*, 1194–1198.

Goldmann, W.H., Hess, D., and Isenberg, G. (1999). The effect of intact talin and talin tail fragment on actin filament dynamics and structure depends on pH and ionic strength. Eur. J. Biochem. *260*, 439–445.

Griffiths, J.R. (1991). Are cancer cells acidic? Br. J. Cancer *64*, 425–427.

Han, J.Y., and Burgess, K. (2010). Fluorescent indicators for intracellular pH. Chem. Rev. *110*, 2709–2728.

Harguindey, S., Orive, G., Luis Pedraz, J., Paradiso, A,, and Reshkin, S.J. (2005). The role of pH dynamics and the Na^+/H^+ antiporter in the etiopathogenesis and treatment of cancer. Two faces of the same coin—one single nature. Biochim. Biophys. Acta *1756*, 1–24.

Izumi, H., Torigoe, T., Ishiguchi, H., Uramoto, H., Yoshida, Y., Tanabe, M., Ise, T., Murakami, T., Yoshida, T., Nomoto, M., and Kohno, K. (2003). Cellular pH regulators: potentially promising molecular targets for cancer chemotherapy. Cancer Treat. Rev. *29*, 541–549.

Jannat, R.A., Robbins, G.P., Ricart, B.G., Dembo, M., and Hammer, D.A. (2010). Neutrophil adhesion and chemotaxis depend on substrate mechanics. J. Phys. Condens. Matter *22*, 194117.

Matthews, B.D., Overby, D.R., Alenghat, F.J., Karavitis, J., Numaguchi, Y., Allen, P.G., and Ingber, D.E. (2004). Mechanical properties of individual focal adhesions probed with a magnetic microneedle. Biochem. Biophys. Res. Commun. *313*, 758–764.

Matthews, B.D., Overby, D.R., Mannix, R., and Ingber, D.E. (2006). Cellular adaptation to mechanical stress: role of integrins, Rho, cytoskeletal tension and mechanosensitive ion channels. J. Cell Sci. *119*, 508–518.

Miller, G.J., and Ball, E.H. (2001). Conformational change in the vinculin C-terminal depends on a critical histidine residue (His-906). J. Biol. Chem. *276*, 28829–28834.

Palecek, S.P., Huttenlocher, A., Horwitz, A.F., and Lauffenburger, D.A. (1998). Physical and biochemical regulation of integrin release during rear detachment of migrating cells. J. Cell Sci. *111*, 929–940.

Palmer, S.M., Schaller, M.D., and Campbell, S.L. (2008). Vinculin tail conformation and self-association is independent of pH and H906 protonation. Biochemistry *47*, 12467–12475.

Putney, L.K., Denker, S.P., and Barber, D.L. (2002). The changing face of the Na^+/H^+ exchanger, NHE1: structure, regulation, and cellular actions. Annu. Rev. Pharmacol. Toxicol. *42*, 527–552.

Riveline, D., Zamir, E., Balaban, N., Kam, Z., Geiger, B., and Bershadsky, A. (1999). Focal contact as mechanosensor: Directional growth in response to local strain. Mol. Biol. Cell Suppl. *10*, 341a.

Sawada, Y., and Sheetz, M.P. (2002). Force transduction by Triton cytoskeletons. J. Cell Biol. *156*, 609–615.

Schmidt, J.M., Zhang, J.W., Lee, H.S., Stromer, M.H., and Robson, R.M. (1999). Interaction of talin with actin: sensitive modulation of filament cross-linking activity. Arch. Biochem. Biophys. *366*, 139–150.

Simchowitz, L., and Cragoe, E.J., Jr. (1986). Regulation of human neutrophil chemotaxis by intracellular pH. J. Biol. Chem. *261*, 6492–6500.

Srivastava, J., Barreiro, G., Groscurth, S., Gingras, A.R., Goult, B.T., Critchley, D.R., Kelly, M.J., Jacobson, M.P., and Barber, D.L. (2008). Structural model and functional significance of pH-dependent talin-actin binding for focal adhesion remodeling. Proc. Natl. Acad. Sci. USA *105*, 14436–14441.

Stock, C., and Schwab, A. (2009). Protons make tumor cells move like clockwork. Pflugers Arch. *458*, 981–992.

Stock, C., Gassner, B., Hauck, C.R., Arnold, H., Mally, S., Eble, J.A., Dieterich, P., and Schwab, A. (2005). Migration of human melanoma cells depends on extracellular pH and Na^+/H^+ exchange. J. Physiol. *567*, 225–238.

Tominaga, T., and Barber, D.L. (1998). Na-H exchange acts downstream of RhoA to regulate integrin-induced cell adhesion and spreading. Mol. Biol. Cell *9*, 2287–2303.

Zamir, E., and Geiger, B. (2001). Molecular complexity and dynamics of cell-matrix adhesions. J. Cell Sci. *114*, 3583–3590.

